Appl. Chem. Eng., Vol. 30, No. 2, April 2019, 133-140
https://doi.org/10.14478/ace.2019.1016

Review

2차원 이황화몰리브덴의 성질, 제조 및 에너지 저장 소자 응용

최봉길†

강원대학교 화학공학과
(2019년 2월 28일 접수, 2019년 3월 4일 심사, 2019년 3월 11일 채택)

Properties, Preparation, and Energy Storage Applications of Two-dimensional Molybdenum Disulfide

Bong Gill Choi†

Department of Chemical Engineering, Kangwon National University, 346 Joongang-ro, Samcheok, Gangwon-do 25913, Republic of Korea
(Received February 28, 2019; Revised March 4, 2019; Accepted March 11, 2019)

Abstract

Two-dimensional (2D) ultrathin molybdenum dichalcogenides MoS_2 has gained a great deal of attention in energy conversion and storage applications because of its unique morphology and property. The 2D MoS_2 nanosheets provide a high specific surface area, 2D charge channel, sub-nanometer thickness, and high conductivity, which lead to high electrochemical performances for energy storage devices. In this paper, an overview of properties and synthetic methods of MoS_2 nanosheets for applications of supercapacitors and rechargeable batteries is introduced. Different phases triangle prismatic 2H and metallic octahedral 1T structured MoS_2 were characterized using various analytical techniques. Preparation methods were focused on top-down and bottom-up approaches, including mechanical exfoliation, chemical intercalation and exfoliation, liquid phase exfoliation by the direct sonication, electrochemical intercalation exfoliation, microwave-assisted exfoliation, mechanical ball-milling, and hydrothermal synthesis. In addition, recent applications of supercapacitors and rechargeable batteries using MoS_2 electrode materials are discussed.

Keywords: *MoS_2, Supercapacitor, Batteries, Composite, Electrochemistry*

1. Introduction

Ever-increasing demand for energy to address depletion of fossil fuels significantly require the development of renewable and sustainable energy storage and conversion systems[1-4]. Rechargeable and storage batteries or secondary cells, can be charged, and discharged into a load, and recharged many times for use, which are designed to deliver high energy and power densities in many energy applications[5-8]. The rechargeable batteries are used in portable electronics and power supplies, electric vehicles, and energy storage power stations, because of their high energy density, low cost, lightweight, size, and long lifetime. A lithium-ion battery is one of the most developed batteries, which consists of anode (*e.g.*, graphite) and cathode (*e.g.*, lithium metal oxide) separated by the electrolyte. Recently, in order to increase energy performance of Li-ion batteries and address limitation of lithium resources, sodium and magnesium-ion batteries have attracted a great deal of attention because of their low cost, natural abundance, and similar insertion mechanism to lithium ions[9-12]. Supercapacitors or electrochemical capacitors store electrical charges by typically two mechanisms: (1) formation of an electrical double layer between electrode and electrolyte and (2) reversible Faradaic reaction at the electrode/electrolyte interface[13,14]. Compared to rechargeable batteries, supercapacitors are capable of delivering higher power density, higher rate capability, and more stable cycle life. However, most supercapacitors suffered from lower energy densities than batteries[15-19].

Ultrathin and layered two-dimensional (2D) nanosheets, especially, graphene materials, have drawn tremendous attention and shown great promise for a wide range of applications[20,21]. Since graphene materials have shown a great potential for the application of energy storage systems, and other 2D materials, such as, metal oxides, hydroxides, dichalcogenides, and carbides have been extensively investigated[22-25]. Among them, molybdenum disulfide (MoS_2) is widely interested in many applications because of its unique 2D morphology and phys-

† Corresponding Author: Kangwon National University, Department of Chemical Engineering, 346 Joongang-ro, Samcheok, Gangwon-do 25913, Republic of Korea
Tel: +82-10-2781-3478 e-mail: bgchoi@kangwon.ac.kr

pISSN: 1225-0112 eISSN: 2288-4505

icochemical properties[26-29]. The 2D morphology enables MoS_2 to provide high specific surface area compared to its bulk counterpart. The ultrathin layers of MoS_2 allow to high flexibility and strong mechanical strength in contrast to MoS_2 bulk materials. The attractive merits of MoS_2 have been demonstrated in many applications of electronics, sensors, and biomedicine. In particular, the high conductivity, large surface area, and active edge sites of MoS_2 made it a promising electrode material for development of energy conversion and storage applications, such as, rechargeable batteries, supercapacitors, electrocatalytic reaction, and solar cells.

In this article, we reviewed unique structures and properties and preparation methods of MoS_2 nanosheets. Various experimental techniques were introduced to investigate MoS_2 nanosheets. We summarized the recent synthetic methods for preparation of MoS_2 materials to achieve nanostructure, extraordinary properties, and enhanced electrochemical performances, including mechanical exfoliation, chemical intercalation and exfoliation, liquid phase exfoliation by direct sonication, electrochemical intercalation exfoliation, microwave-assisted exfoliation, mechanical ball-milling, and hydrothermal synthesis. Following that, the main applications of MoS_2 materials are reviewed, involving energy storage systems of supercapacitors and rechargeable batteries.

2. Properties of MoS_2

Natural MoS_2 materials have a crystalline structure of trigonal prismatic or an octahedral Mo coordination[30]. Particularly, MoS_2 has different polymorphs depending on the electron filling in the valence d-orbitals of Mo atoms, involving 3R of rhombohedral polymorph with three-layers and Mo atoms in trigonal prismatic coordination, 2H of hexagonal with two-layers and Mo atoms in trigonal prismatic coordination, and 1T of trigonal with one-layer and Mo atoms in octahedral coordination[31]. MoS_2 shows diverse electrical and optical properties according to the different atomic arrangement of MoS_2. The 2H MoS_2 is naturally abundant and stable, and exhibits indirect bandgap of 1.29 eV for bulk state and direct bandgap of 1.90 eV for monolayer state[32]. The 1T MoS_2 shows hydrophilic and metallic nature; the electrical conductivity of 1T is 10^7 times higher than 2H phase. The 1T MoS_2 has a similar electrical conductivity with metallic materials of copper and gold. The attractive features of 1T MoS_2 have made it as a promising electrode material in applications of energy storage and conversion.

The transformation of 2H into 1T phase in MoS_2 can be characterized by various analytical techniques, such as, X-ray diffraction (XRD), X-ray photoelectron spectroscopy (XPS), transmission electron microscopy (TEM), Raman, photoluminescence (PL), extended X-ray absorption fine structure (EXAFS), and ultraviolet-visible (UV-vis)[30]. The measurement of XRD using bulk 2H MoS_2 and 1T MoS_2 samples provides exfoliation states and crystalline structure of MoS_2. The exfoliated 1T MoS_2 compared to 2H MoS_2 exhibits reduced (002) peak with blue shift, indicating expansion of the interlayer spacing and low crystallinity. In addition, most XRD peaks of 1T MoS_2 are reduced when MoS_2 sheets are exfoliated. Raman spectroscopy provides a clear evidence for the formation of 1T phase MoS_2. The 2H MoS_2 shows characteristic peaks of 380 cm^{-1} (E^1_{2g} mode associated with opposite vibration of two S atoms with respect to the Mo atom) and 400 cm^{-1} (A^1_g mode associated with the vibration of only S atoms in opposite directions)[30]. Compared to 2H MoS_2, the 1T MoS_2 shows prominent peaks at around 150, 220, 280, 330, and 400 cm^{-1}, corresponding J_1, J_2, E^1_g, J_3, and A^1_g modes, respectively. As the 1T phase increases, E^1_g, and A^1_g decrease, while J_1, J_2, and J_3 modes increase[30]. This observation in Raman spectroscopy indicates the presence of the as-synthesized 1T phase in MoS_2 sheets. The atomic arrangement of Mo and S between the triangle prismatic and octahedral coordination structures differ from each other. Hence, Mo 3d and S 2p XPS investigation is one of the most promising way to detect 1T phase of MoS_2. In addition, peak fitting of Mo 3d and S 2p XPS provides accurate 1T contents of MoS_2. The different atomic structures of MoS_2 result in different optical properties, and thus UV-vis absorption spectrum of 2H MoS_2 and 1T MoS_2 are a good indicator to distinguish phases of MoS_2. Typically, 2H MoS_2 shows three peaks at 440 (attributed to the quantum effect of small lateral-sized MoS_2 sheets), 610, and 650 nm (attributed to the energy split large lateral dimensions)[33]. The formation of 1T phase removes the characteristic peaks of 2H MoS_2, indicating metallic properties of 1T MoS_2.

3. Preparation of MoS_2

Tremendous efforts have been attempted to synthesize MoS_2 nanosheets in terms of production cost and scalability. Various methods have been employed to prepare MoS_2 in order to achieve nanostructure, special properties, and superior performance, including mechanical exfoliation, chemical intercalation and exfoliation, liquid phase exfoliation by direct sonication, electrochemical intercalation exfoliation, microwave-assisted exfoliation, mechanical ball-milling, and hydrothermal synthesis[34-46].

3.1. Top-down approaches for preparation of MoS_2

Similar to graphene materials, MoS_2 nanosheets can be obtained from mechanical exfoliation of bulk layered MoS_2 powers. Novoselov and co-workers successfully exfoliated MoS_2 into single-layer MoS_2 nanosheet with a high quality of crystalline structure and micro-sized lateral size, but the very small quantities are limited to many practical applications[36]. In order to enhance production rate of MoS_2 nanosheets, lithium ion-intercalation and exfoliation methods have extensively been developed[38,39]. Typically, this process is carried out in an atmosphere protected by inert gas, such as, an argon-filled glove box, using *n*-butyl-lithium at a certain temperature for a certain time of 5~70 h (Figure 1). The lithium-ion intercalation can be accelerated by the assistance of sonication, microwaves, and ball-milling. And also, a lithium-ion battery system was attempted to intercalate Li-ion into layered MoS_2 sheets, in which bulk MoS_2 and lithium foil were used as the cathode and anode, respectively[37]. By discharging, Li-ion effectively intercalates into bulk MoS_2 sheets, thereby achieving efficient exfoliation of MoS_2. Other alkali metals have been employed to exfoliate MoS_2. The use of alkali metals as the intercalants are basically

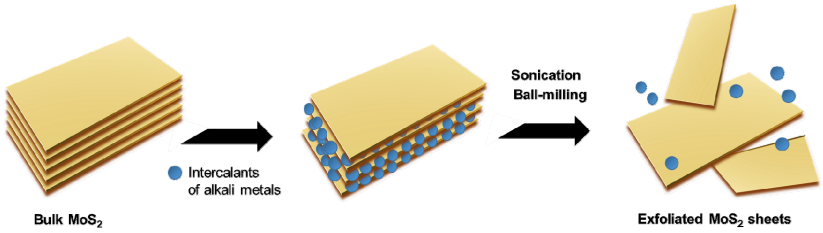

Figure 1. Schematic illustration of exfoliation of MoS_2 using alkali metals as intercalants and post-treatments of sonication and ball milling methods.

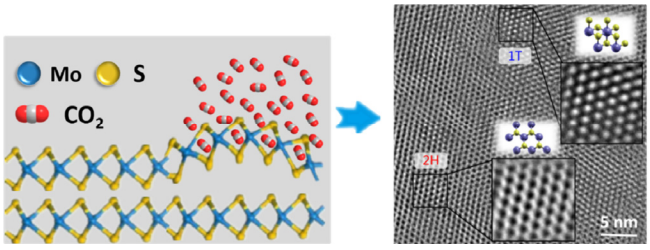

Figure 2. Schematic illustration of adsorption of CO_2 on the single-layer MoS_2 and TEM image of 1T and 2H phases of MoS_2 sheet (Reprinted with permission form ref. 42. Copyright (2016) American Chemical Society).

electron donors, and thus inducing strain force by the electron transfer from the intercalant. The strain force leads to facilitate the phase transition of MoS_2 from 2H to 1T[34]. Compared to 2H MoS_2, 1T MoS_2 exhibits higher electrical conductivity, larger spacing distance, and more abundant active site surfaces. These features of 1T MoS_2 are especially favorable to the electrochemical applications that require high electron and ion conductivity. The 1T phase of MoS_2 was confirmed by various analytical instruments, such as, TEM, XRD, Raman, STEM, and XPS.

On the other hand, other top-down approaches have been developed. The mechanical ball-milling process can be used to prepare MoS_2 nanosheets without any additives or any other additional treatment for several hours. In particular, the milling time influenced the size of MoS_2 and phase transition (2H to 1T)[40]. The use of microwaves was also reported by Reshmi *et al.* for exfoliating MoS_2 and phase conversion of 2H into 1T[41]. Recently, supercritical CO_2-assisted exfoliation method has been also developed by Xu and coworkers (Figure 2)[42]. The use of supercritical CO_2 gas effectively exfoliated bulk MoS_2 into mono- or few-layer MoS_2 nanosheets. The pre-dispersion of MoS_2 flakes in a mixture of ethanol and water was treated in supercritical CO_2 gas condition at 80 ℃ and 16 MPa under stirring for 6 h. The introduction of CO_2 gas induced stain forces into MoS_2 sheets, and thus leading to phase transform of the 2H into the 1T phase of MoS_2. Because the 1T phase of MoS_2 is important in applications of electrochemical devices, numerous methods have been developed to control the phase of MoS_2. The phase transition of 2H and 1T can be occurred by mechanical tensile and compressive strains onto the MoS_2 surfaces. Chi *et al.* reported that high pressure up to 81 GPa induced sufficient strain forces into MoS_2 sheets, and thus leading to 1T phase by mechanical layer sliding[43]. However, this compressive pressure is extremely high and the process is very low throughput, which is hard to realize. In order to induce phase transition of 2H into 1T, electron injection, argon-plasma treatment, and chemical vapor treatment have successfully developed. More recently, our group reported scalable and straightforward process for exfoliating MoS_2 materials using fluid dynamins into metallic MoS_2 sheets, resulting in an impressive yield performance of 76.9% and a high concentration of 20 mg/mL[35]. In this process, ionic liquid was used as additives for stabilizing MoS_2 dispersion and 1T phase.

3.2. Bottom-up approaches for preparation of MoS_2

Hydrothermal and solvothermal reactions are common for preparing MoS_2 nanosheets[44-46]. A mixture of ammonium molybdate tetrahydrate ($(NH_4)_6Mo_7O_{24}\cdot 4H_2O$) and thiourea was used as the precursors for the Mo and S elements. The precursors were thermally treated at 200 ℃ for 20 h. The typically obtained MoS_2 sheets have a lateral size of 200 nm with 2~5 layers. In addition, 1T phase of MoS_2 was also obtained with 1T contents of < 70%. In order to increase 1T contents, the temperature-assisted phase transform of MoS_2 has been developed. The hydrothermal treatment at 180 ℃ for 24 h induced metallic phase up to 92.4%. The high temperature above 200 ℃ caused to the formation of dominant 2H phase (> 90%). The composition ratio of precursors is also critical factor for control the phase of MoS_2. Liu *et al.* reported that changing the precursor ratio significantly influenced metallic contents of MoS_2[45].

4. Applications of MoS_2

Since the 2H MoS_2 was synthesized for many applications, the 1T MoS_2 has also synthesized and now been widely used in various application fields, such as, electrocatalysts (Figure 3), electronic devices, photovoltaic, sensors, and energy storage and conversion systems[27,34].

4.1. Supercapacitor

Supercapacitors, also called ultracapacitors or electrochemical capacitors, are power supply devices to bridge the gap between batteries and capacitors[1-10]. By separating electrolyte ions, supercapacitors can store electrical charges and provides high power density. The desirable supercapacitors can operate at high charge and discharge rates within a few seconds during long-term. Recent issue of supercapacitors is how to increase energy densities, which is generally low than lithium-ion batteries. Since the discovery of graphene materials, ultra

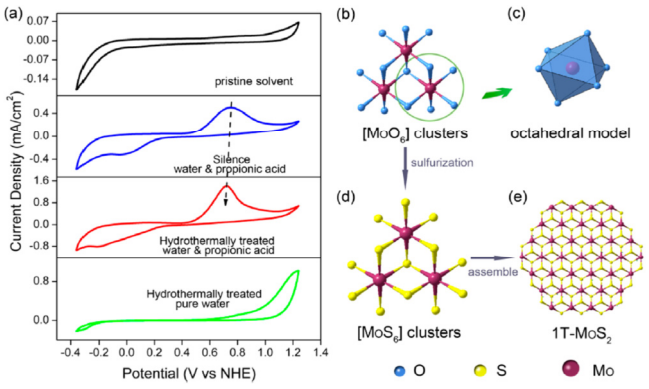

Figure 3. (a) Cyclic voltammograms of various solutions. (b)~(e) Schematic illustrations for the evolution process of the 1T phase based on Mo (Reprinted with permission form ref. 46. Copyright (2017) American Chemical Society).

thin-layered 2D materials are promising electrode materials to achieve a high capacitance, resulting in high energy density of supercapacitors [5]. Various 2D materials, including MXenes, metal oxides, metal hydroxides, and disulfide family, have been extensively attempted to enhance electrochemical performances of supercapacitors[5]. Among them, MoS_2 has been attracted a great deal of attention for development of supercapacitors because of its high theoretical capacitance value and unique structural properties of MoS_2. The porous MoS_2 thin films were prepared by Choudhary and coworkers based on a direct magnetron sputtering method[47]. The MoS_2 film electrode showed a high gravimetric capacitance of 330 F/g at 10 V/s (high rate capability) and a good cycling stability of 97% retention over 5,000 cycles of charging/discharging measurement. Karade *et al.* synthesized ultrathin and layer MoS_2 nanosheets by a chemical deposition method, and demonstrated as energy storage electrodes by a high specific capacitance of 576 F/g at 5 mV/s and an excellent cycle life (82% retention over 3000 cycles)[48]. However, 2H MoS_2 electrodes limited to practical supercapacitor electrodes because of their poor electrical conductivity. In contrast, the metallic MoS_2 electrodes provide more advantages of high electrical conductivity, a high hydrophilicity, and a large interlayer space. Acerce and coworkers successfully fabricated 1T MoS_2 film electrodes by a chemical intercalation-exfoliation and post vacuum filtration methods[49]. The 1T MoS_2 film electrode had a thickness of 5 μm and film packing density of 2.5 mg/cm^2, in which 1T content is approximately 70%. The 1T MoS_2 film electrode showed an extremely high volumetric capacitance of 400~650 F/cm^3 at a scan rate of 20 mV/s. In addition, this MoS_2 film electrode had high specific capacitance at high scan rate of 200 mV/s. Hence, high energy and power densities were achieved to 0.11 Wh/cm^3 and 1.1 W/cm^3, respectively. Other researchers have focused on synthesis of 1T MoS_2 materials and applied them into supercapacitor electrodes. Thi *et al.* reported that synthesized 1T MoS_2 nanoflower-based electrodes show a high specific capacitance of 259 F/g at 5 mV/s with a good long-term stability during 1,000 cycles[50]. On the other hand, MoS_2/carbon composite electrodes have been developed in order to address intrinsically low electrical conductivity of MoS_2. Various nanocarbon materials have been employed, including carbon nanofibers, graphene, carbon nanotubes, carbon spheres, and conducting polymers. Huang and coworkers synthesized composite electrodes consisted of carbon aerogel/MoS_2, showing 260 F/g at 1 A/g with a good cycle life of 924% capacitance retention over 1,500 cycles[51]. The MoS_2/graphene-incorporated into multiwalled carbon nanotube electrodes have been also prepared, showing a high specific capacitance, a high rate capability, and a good long-term stability. To increase ion and electron transport properties in electrode materials, three-dimensional (3D) MoS_2/graphene aerogel composites were synthesized by a self-assembly of graphene oxide under hydrothermal treatment. As-synthesized 3D MoS_2/graphene electrodes showed a high capacitance of 231 F/g with high energy (26 Wh/kg) and power (6,443 W/kg) densities[52]. Zhang and coworkers fabricated a rambutan-like composite electrode of MoS_2-incorporated into carbon spheres[53]. This composite electrode exhibited a high specific capacitance of 411 F/g at an applied current density of 1 A/g and a good long-term stability of 93.2% capacitance retention during 1,000 cycles. The conducting polymers have been also attempted to enhance the electrical conductivity of MoS_2. For instance, poly(3,4-ethylenedioxythiophene) was *in situ* polymerized onto the MoS_2 surface. The coated conducting polymer enhanced the electrochemical performance of composite electrodes, showing a high specific capacitance of 405 F/g and an excellent capacitance retention of 90% over 1,000 cycles[54]. Yang *et al.* synthesized core-shell structured electrode consisted of polyaniline shell and 1T MoS_2 core. This unique structured electrode exhibited an impressive specific capacitance of 678 F/g at 1 mV/s with a good capacitance retention of 80% during 10,000 cycles[55]. The polypyrrole was polymerized onto the MoS_2 surface, showing a high specific capacitance of 700 F/g at a scan rate of 10 mV/s and a good cycling stability of 85% capacitance retention during 4,000 cycles[56]. The controlled morphology of conducting polymer/MoS_2 composite electrodes showed enhanced electrochemical performances for supercapacitor applications. The Mn_3O_4 was incorporated into MoS_2 using a hydrothermal and chemical precipitation method. This hybrid electrode showed a high specific capacitance of 119.3 F/g after 2,000 cycles at an applied current density of 1 A/g with a capacitance retention of 69.3%[57]. The ultrathin layered 2D hybrid films of graphene/MoS_2 was fabricated by vacuum filtration method, showing an extremely high volumetric capacitance of 1,292.0 F/cm^3 at 1 A/g and an excellent cycle life[58].

4.2. Rechargeable batteries

Increasing energy demands in modern society has required the development of the high energy and power density of energy devices. Lithium-ion batteries have offered high energy densities for commercially available electronic products, such as, personal mobile phones, notebooks, portable electronics, and electric or hybrid vehicles[59]. They can store electrical charges by the electrochemical reactions between anode and cathode materials. Graphite is one of the most promising anode materials in commercial Li-ion batteries. However, the intrinsically low theoretical capacity of graphite (372 mAh/g) limited to application of Li-ion batteries. In this regard, MoS_2 has been attracted

much attention as anode materials for development of lithium ion batteries because of its high theoretical capacity of 670 mAh/g, low cost, and natural abundance. The 2D layer structure of MoS_2 allows accumulating Li^+, Na^+, and Mg^{2+} ions. Despite of these attractive features of MoS_2 in battery applications, MoS_2-based electrodes suffered from poor stability and low rate capability originated from formation of Li_2S after the first cycle[60]. Thus, recent researches focused on high rate capability and long-term stability of MoS_2-based electrodes for lithium ion batteries.

Various morphologies and structures of MoS_2 materials have been fabricated. For instance, Xu *et al.* reported that 3D microspheres of MoS_2 nanoflakes through a solid phase reaction method show a high discharge capacity of 850.9 mAh/g at 100 mA/g over 50 cycles[61]. The 2D MoS_2 nanosheet electrodes synthesized by Veeramalai and coworkers showed 1,097 mAh/g at 50 mA/g after 25 cycles[62]. In addition, 3D hierarchical structured MoS_2 with porous structure prepared by Wang *et al.* exhibited a discharge capacity of 845 mAh/g at 100 mA/g after 50 cycles with a good stability even at a high rate of 500 mA/g over 100 cycles[63]. The MoS_2-based electrodes suffered from low electrical conductivity. Hence, 1T MoS_2 has been intensively investigated because of its high electrical conductivity and expanded interlayer space. The pristine 2H MoS_2 typically exhibited 600 mAh/g at the first cycle and decreased dramatically to ~200 mAh/g in the second cycle. In contrast, 1T MoS_2 delivered as high as specific capacity of 1,000 mA/g and maintained 50% retention after 50 cycles. In order to address the issues of MoS_2-based electrodes, carbon materials have incorporated into electrode materials[34]. The graphene/MoS_2 composites with 2H and 1T hybrid phase through a hydrothermal synthesis showed a high discharge capacity of 1,086 mAh/h at 500 mA/g and a high capacity retention of 82.6% (897 mAh/g) after 50 cycles[64]. The sandwich-structured MoS_2/graphene composite electrodes exhibited an extremely high specific capacity of 1,800 mA even at a high rate of 1 A/g. The controlled solvothermal method enabled to deposition of MoS_2 nanosheets onto the carbon cloth surface, showing 1,789 mAh/g at 0.1 A/g and 853 mAh/g after 140 cycles[65]. In addition, nitrogen-doped MoS_2 deposited onto carbon cloth delivered a high discharge capacity of 1,308 mAh/g at 0.1 A/g and 1,125 mAh/g after 100 cycles[66]. The MoS_2 was incorporated into metal oxides, such as, TiO_2. Chen *et al.* reported that 3D porous MoS_2/TiO_2 nanocomposite electrodes showed an excellent cycling performance of 95.9% retention after 100 cycles[67].

Apart from lithium ion batteries, MoS_2 was used as an electrode material for application of lithium-sulfur batteries. Compared to lithium ion batteries, Li-S batteries provide higher energy density (2,800 Wh/kg) and higher theoretical capacity of 1,675 mAh/g. However, Li-S batteries suffered from the intrinsically low electrical conductivity of sulfur, the formation of polysulfides, and significant volume expansion. To address these issues, Wang *et al.* described that hierarchical and porous structured SnO_2/1T MoS_2 nanosheets deposited onto the carbon cloth surface showed 448 mAh/g after 4,000 cycles[68]. Jeong and coworkers fabricated 1T MoS_2 and carbon nanotube composite electrode, showing 670 mAh/g after 500 cycles at a high rate of 1C[69]. The availability of MoS_2 sheets with the intercalation of alkali metal ions allowed them to accumulate sodium ions among the MoS_2 sheets, resulting in fabrication of Na-ion batteries. The graphene/MoS_2 composite electrodes exhibited a high rate capability of 284 mAh/g at a high rate of 20 A/g with an excellent cycle life of 95% retention after 250 cycles[70]. In addition, expanding MoS_2 sheets with polyethylene oxide led to a high specific capacity of 225 mAh/g and maintained 148 mAh/g after 70 cycles[71]. Because the magnesium can accumulate charges two times higher than those of sodium and lithium metal, magnesium ion batteries have been attracted a great deal of attention as potential rechargeable energy storage devices. Liang and coworkers reported that MoS_2/polyethylene oxide composite electrodes exhibited a specific capacity of 75 mAh/g at 5 mA/g[72]. In addition, Liu *et al.* fabricated graphene/MoS_2 composite electrode, showing a high discharge capacity of 115.9 mAh/g and a good cycle life of 82.5 mAh/g after 50 cycles[73].

5. Conclusions

We summarized the properties, preparation methods, and energy storage applications of MoS_2 materials. Particularly, the properties of MoS_2 depend on morphologies and phase. Thus, various synthetic methods of MoS_2 were introduced involving top-down and bottom-up approaches. Supercapactors and rechargeable batteries (*i.e.*, lithium-ion, magnesium-ion, and sodium-ion batteries) using MoS_2 electrode materials were described. The metallic MoS_2 nanosheets have showed a promising potential in energy storage applications, because of their high electrical conductivity, hydrophilicity, high active surface area, and expanded interlayer distance. Although MoS_2 materials has been employed as advanced electrode materials in energy storage field, there still are many challenges in terms of mass production, fine control of phase and morphology, and unit cost production.

Acknowledgment

This work was supported by the National Research Foundation of Korea (NRF) Grant funded by the Ministry of Science and ICT (grant no. 2018R1A2A3075668).

References

1. M. R. Lukatskaya, B. Dunn, and Y. Gogotsi, Multidimensional materials and device architectures for future hybrid energy storage, *Nat. Commun.*, **7**, 12647-12659 (2016).
2. M. Salanne, B. Rotenber, K. Naoi, K. Kaneko, P.-L. Taberna, C. P. Grey, B. Dunn, and P. Simon, Efficient storage mechanisms for building better supercapacitors, *Nat. Energy*, **1**, 16070-16079 (2016).
3. P. Simon, Y. Gogotsi, and B. Dunn, Where do batteries end and supercapacitors begin?, *Science*, **343**, 1210-1211 (2014).
4. G. Z. Chen, Supercapacitor and supercapattery as emerging electrochemical energy stores, *Int. Mater. Rev.*, **62**, 173-202 (2017).
5. X. Xiao, H. Wang, P. Urbankowski, and Y. Gogotsi, Topochemical synthesis of 2D materials, *Chem. Soc. Rev.*, **47**, 8744-8765 (2018).

6. X. Ke, J. M. Prahl, J. I. D. Alexander, J. S. Wainright, T. A. Zawodzinski, and R. F. Savinell, Rechargeable redox flow batteries: Flow fields, stacks and design considerations, *Chem. Soc. Rev.*, **47**, 8721-8743 (2018).
7. Q. Wang, L. Jiang, and J. Sun, Progress of enhancing the safety of lithium ion battery from the electrolyte aspect, *Nano Energy*, **55**, 93-114 (2019).
8. P. Zhang, F. Wang, M. Yu, X. Zhuang, and X. Feng, Two-dimensional materials for miniaturized energy storage devices: From individual devices to smart integrated systems, *Chem. Soc. Rev.*, **47**, 7426-7451 (2018).
9. F. Zou, Y.-M. Chen, K. Liu, Z. Yu, W. Liang, S. M. Bhaway, M. Gao, and Y. Zhu, Metal organic frameworks derived hierarchical hollow NiO/Ni/graphene composites for lithium and sodium storage, *ACS Nano*, **10**, 377-386 (2016).
10. Y. Zou, X. Rui, W. Sun, Z. Xu, Y. Zhou, W. J. Ng, Q. Yan, and E. Fong, Biochemistry-enabled 3D foams for ultrafast battery cathodes, *ACS Nano*, **9**, 4628-4635 (2015).
11. A. J. Crowe, K. K. Stringham, J. L. Dimeglio, and B. M. Bartlett, Adsoprtion of aromatic decomposition products from phenyl-containing magnesium-ion battery electrolyte solutions, *J. Phys. Chem. C*, **121**, 7711-7717 (2017).
12. Y.-H. Tan, W.-T. Yao, T. Zhang, T. Ma, L.-L. Lu, F. Zhou, H.-B. Yao, and S.-H. Yu, High voltage magnesium-ion battery enabled by nanocluster Mg_3Bi_2 alloy anode in noncorrosive electrolyte, *ACS Nano*, **12**, 5856-5865 (2018).
13. J. Sun, C. Wu, X. Sun, H. Hu, C. Zhi, L. Houa, and C. Yuan, Recent progresses in high-energy-density all pseudocapacitive-electrode-materials-based asymmetric supercapacitors, *J. Mater. Chem. A*, **5**, 9443-9464 (2017).
14. N. Choudhary, C. Li, J. Moore, N. Nagaiah, L. Zhai, Y. Jung, and J. Thomas, Asymmetric supercapacitor electrodes and devices, *Adv. Mater.*, **29**, 1605336-1605365 (2017).
15. H. Wu and K. Lian, Aqueous based asymmetrical-bipolar electrochemical capacitor with a 2.4 V operating voltage, *J. Power Sources*, **378**, 209-215 (2018).
16. K. Nueangnoraj, R. Ruiz-Rosas, H. Nishihara, S. Shiraishi, E. Morallón, D. Cazorla-Amorós, and T. Kyotani, Carbon-carbon asymmetric aqueous capacitor by pseudocapacitive positive and stable negative electrodes, *Carbon*, **67**, 792-794 (2018).
17. J.-G. Wang, Y. Yang, Z.-H. Huang, and F. Kang, A high-performance asymmetric supercapacitor based on carbon and carbon-MnO_2 nanofiber electrodes, *Carbon*, **61**, 190-199 (2013).
18. M. Yang, K. G. Lee, S. J. Lee, S. B. Lee, Y.-K. Han, and B. G. Choi, Three-dimensional expanded graphene-metal oxide film via solid-state microwave irradiation for aqueous asymmetric supercapacitors, *ACS Appl. Mater. Interfaces*, **7**, 22364-22371 (2015).
19. F. Wang, S. Xiao, Y. Hou, C. Hu, L. Liu, and Y. Wu, Electrode materials for aqueous asymmetric supercapacitors, *RSC Adv.*, **3**, 13059-13084 (2013).
20. Q. Wang, J. Yan, and Z. Fan, Carbon materials for high volumetric performance supercapacitors: Design, progress, challenges and opportunities, *Energy Environ. Sci.*, **9**, 729-762 (2016).
21. B. Mendoza-Sánchez and Y. Gogotsi, Synthesis of two-dimensional materials for capacitive energy storage, *Adv. Mater.*, **28**, 6104-6135 (2016).
22. Y. Chen, W. K. Pang, H. Bai, T. Zhou, Y. Liu, S. Li, and Z. Guo, Enhanced structural stability of nickel-cobalt hydroxide via intrinsic pillar effect of metaborate for high-power and long-life supercapacitor electrodes, *Nano Lett.*, **17**, 429-436 (2016).
23. C. Couly, M. Alhabeb, K. L. Van Aken, N. Kurra, L. Gomes, A. M. Navarro-Suárez, B. Anasori, H. N. Alshareef, and Y. Gogotsi, Asymmetric flexible MXene-reduced graphene oxide micro-supercapacitor, *Adv. Electron. Mater.*, **4**, 1700339-1700357 (2018).
24. Z. Lei, J. Zhang, and X. S. Zhao, Ultrathin MnO_2 nanofibers grown on graphitic carbon spheres as high-performance asymmetric supercapacitor electrodes, *J. Mater. Chem.*, **22**, 153-160 (2012).
25. F. Ghasemi, M. Jalali, A. Abdollahi, S. Mohammadi, Z. Sanaee, and Sh. Mohajerzadeh, A high performance supercapacitor based on decoration of MoS_2/reduced graphene oxide with NiO nanoparticles, *RSC Adv.*, **7**, 52772-52781 (2017).
26. K. S. Kumar, N. Choudhary, Y. Jung, and J. Thomas, Recent advances in two-dimensional nanomaterials for supercapacitor electrode applications, *ACS Energy Lett.*, **3**, 482-495 (2018).
27. W.-J. Zhang and K.-J. Huang, A review of recent progress in molybdenum disulfide-based supercapacitors and batteries, *Inorg. Chem. Front.*, **4**, 1602-1620 (2017).
28. T. Wang, S. Chen, H. Pang, H. Xue, and Y. Yu, MoS_2-based nanocomposites for electrochemical energy storage, *Adv. Sci.*, **4**, 1600289-1600315 (2017).
29. Z. S. Iro, C. Subramani, and S. S. Dash, A brief review on electrode materials for supercapacitor, *Int. J. Electrochem. Sci.*, **11**, 10628-10643 (2016).
30. G. Zhang, H. Liu, J. Qu, and J. Li, Two-dimensional layered MoS_2: Rational design, properties and electrochemical applications, *Energy Environ. Sci.*, **9**, 1190-1209 (2016).
31. M. Chhowalla, H. S. Shin, G. Eda, L.-J. Li, K. P. Loh, and H. Zhang, The chemistry of two-dimensional layered transition metal dichalcogenides nanosheets, *Nat. Chem.*, **5**, 263-275 (2013).
32. B. Hinnemann, P. G. Moses, J. Bonde, K. P. Jorgensen, J. H. Nielsen, S. Horch, I. Chorkendorff, and J. K. Norskov, Biomimetic hydrogen evolution: MoS_2 nanoparticles as catalyst for hydrogen evolution, *J. Am. Chem. Soc.*, **127**, 5308-5309 (2005).
33. S. Tongay, J. Zhou, C. Ataca, K. Lo, T. S. Mattenws, J. Li, J. C. Grossman, and J. Wu, Thermally driven crossover from indirect toward direct bandgap in 2D semiconductors: $MoSe_2$ versus MoS_2, *Nano Lett.*, **12**, 5576-5580 (2012).
34. S. Shi, Z. Sun, and Y. H. Hu, Synthesis, stabilization and applications of 2-dimensional 1T metallic MoS_2, *J. Mater. Chem. A*, **6**, 23932-23977 (2018).
35. J.-M. Jeong, H. G. Kang, H.-J. Kim, S. B. Hong, H. Jeon, S. Y. Hwang, D. Seo, B. E. Kwak, Y.-K. Han, B. G. Choi, and D. H. Kim, 2D nanosheets: hydraulic power manufacturing for highly scalable and stable 2D nanosheet dispersions and their film electrode application, *Adv. Funct. Mater.*, **28**, 1802952-1802964 (2018).
36. K. S. Novoselov, D. Jiang, F. Schedin, T. J. Booth, V. V. Khotkevich, S. V. Morozov, and A. K. Geim, Two-dimensional atomic crystals, *Proc. Natl. Acad. Sci. U.S.A.*, **102**, 10451-10453 (2005).
37. Z. Zeng, Z. Yin, X. Huang, H. Li, Q. He, G. Lu, F. Boey, and H. Zhang, Single-layer semiconducting nanosheets: High-yield preparation and device fabrication, *Angew. Chem., Int. Ed.*, **50**, 11093-11097 (2011).
38. P. Joensen, R. F. Frindt, and S. R. Morrison, Single-layer MoS_2, *Mater. Res. Bull.*, **21**, 457-461 (1986).

39. Z. Zeng, T. Sun, J. Zhu, X. Huang, Z. Yin, G. Lu, Z. Fan, Q. Yan, H. H. Hng, and H. Zhang, An effective method for the fabrication of few-layer-thick inorganic nanosheets, *Angew. Chem. Int. Ed.*, **51**, 9052-9056 (2012).
40. P. Cheng, K. Sun, and Y. H. Hu, Mechanically-induced reverse phase transformation of MoS_2 from stable 2H to metastable 1T and its memristive behavior, *RSC Adv.*, **6**, 65691-65697 (2016).
41. S. Reshmi, M. V. Akshaya, B. Satpati, P. K. Basu, and K. Bhattacharjee, Structural stability of coplanar 1T-2H superlattice MoS_2 under high energy electron beam, *Nanotechnology*, **29**, 205604-205616 (2018).
42. Y. Qi, Q. Xu, Y. Wang, B. Yan, Y. Ren, and Z. Chen, CO_2-induced phase engineering: Protocol for enhanced photoelectrocatalytic performance of 2D MoS_2 nanosheets, *ACS Nano*, **10**, 2903-2909 (2016).
43. Z. H. Chi, X. M. Zhao, H. Zhang, A. F. Goncharov, S. S. Lobanov, T. Kagayama, M. Sakata, and X. J. Chen, Pressure-induced metallization of molybdenum disulfide, *Phys. Rev. Lett.*, **113**, 036802-036805 (2014).
44. X. Geng, W. Sun, W. Wu, B. Chen, A. Al-Hilo, M. Benamara, H. Zhu, F. Watanabe, J. Cui, and T. Chen, Pure and stable metallic phase molybdenum disulfide nanosheets for hydrogen evolution reaction, *Nat. Commun.*, **7**, 10672-10679 (2016).
45. Q. Liu, X. L. Li, Q. He, A. Khalil, D. B. Liu, T. Xiang, X. J. Wu, and L. Song, Gram-scale aqueous synthesis of stable few-layered 1T-MoS_2: Applications for visible-light-driven photocatalytic hydrogen evolution, *Small*, **11**, 5556-5564 (2015).
46. Z. P. Liu, Z. C. Gao, Y. H. Liu, M. S. Xia, R. W. Wang, and N. Li, Heterogeneous nanostructure based on 1T-phase MoS_2 for enhanced electrocatalytic hydrogen evolution, *ACS Appl. Mater. Interfaces*, **9**, 25291-25297 (2017).
47. N. Choudhary, M. Patel, Y. H. Ho, N. B. Dahotre, W. Lee, J. Y. Hwang, and W. Choi, Directly deposited MoS_2 thin film electrodes for high performance supercapacitors, *J. Mater. Chem. A*, **3**, 24049-24054 (2015).
48. S. S. Karade, D. P. Dubal, and B. R. Sankapal, MoS_2 ultrathin nanoflakes for high performance supercapacitors: Room temperature chemical bath deposition (CBD), *RSC Adv.*, **6**, 39159-39165 (2016).
49. M. Acerce, D. Voiry, and M. Chhowalla, Metallic 1T phase MoS_2 nanosheets as supercapacitor, *Nat. Nanotechnol.*, **10**, 313-318 (2015).
50. N. Thi Xuyen and J. M. Ting, Hybridized 1T/2H MoS_2 having controlled 1T concentrations and its use in supercapacitors, *Chem. Eur. J.*, **23**, 17348-17355 (2017).
51. K. J. Huang, L. Wang, J. Z. Zhang, and K. Xing, MoS_2-based nanocomposites for electrochemical energy storage, *J. Electroanal. Chem.*, **752**, 33-40 (2015).
52. T. N. Y. Khawula, K. Raju, P. J. Franklyn, L. Sigalas, and K. I. Ozoemena, Symmetric pseudocapacitors based on molybdenum disulfide (MoS_2)-modified carbon nanospheres: Correlating physicochemistry and synergistic interaction on energy storage, *J. Mater. Chem. A*, **4**, 6411-6425 (2016).
53. Y. Zhang, T. He, G. Liu, L. Zu, and J. Yang, One-pot mass preparation of MoS_2/C aerogels for high-performance supercapacitors and lithium-ion batteries, *Nanoscale*, **9**, 10059-10066 (2017).
54. J. Wang, Z. Wu, H. Yin, W. Li, and Y. Jiang, Poly(3,4-ethylenedioxythiophene)/MoS_2 nanocomposites with enhanced electrochemical capacitance performance, *RSC Adv.*, **4**, 56926-56932 (2014).
55. C. Yang, Z. Chen, I. Shakir, Y. Xu, and H. Lu, Rational synthesis of carbon shell coated polyaniline/MoS_2 monolayer composites for high-performance supercapacitors, *Nano Res.*, **9**, 951-962 (2016).
56. Q. Pan, F. Zheng, X. Ou, C. Yang, X. Xiong, Z. Tang, L. Zhao, and M. Liu, MoS_2 decorated $Fe_3O_4/Fe_{1-x}S$@C nanosheets as high-performance anode materials for lithium ion and sodium ion batteries, *ACS Sustain. Chem. Eng.*, **5**, 4739-4745 (2017).
57. M. Wang, H. Fei, P. Zhang, and L. Yin, Hierarchically layered MoS_2/Mn_3O_4 hybrid architectures for electrochemical supercapacitors with enhanced performance, *Electrochim. Acta*, **209**, 389-398 (2016).
58. H. Jeon, J.-M. Jeong, H. G. Kang, H.-J. Kim, J. Park, D. H. Kim, Y. M. Jung, S. Y. Hwang, Y.-K. Han, and B. G. Choi, Scalable water-based production of highly conductive 2D nanosheets with ultrahigh volumetric capacitance and rate capability, *Adv. Energy. Mater.*, **8**, 1800227-1800238 (2018).
59. D. Xie, D. H. Wang, W. J. Tang, X. H. Xia, Y. J. Zhang, X. L. Wang, C. D. Gu, and J. P. Tu, Binder-free network-enabled MoS_2-PPY-rGO ternary electrode for high capacity and excellent stability of lithium storage, *J. Power Sources*, **307**, 510-518 (2016).
60. S. Zhang, B. V. R. Chowdari, Z. Wen, J. Jin, and J. Yang, Constructing highly oriented configuration by few-layer MoS_2: Toward high-performance lithium-ion batteries and hydrogen evolution reactions, *ACS Nano*, **9**, 12464-12472 (2015).
61. J. Xu, H. Tang, Y. Chu, and C. Li, Facile synthesis and electrochemical properties of MoS_2 nanostructures with different lithium storage properties, *RSC Adv.*, **5**, 48492-48499 (2015).
62. C. P. Veeramalai, F. Li, H. Xu, T. W. Kimb, and T. Guo, One pot hydrothermal synthesis of graphene like MoS_2 nanosheets for application in high performance lithium ion batteries, *RSC Adv.*, **5**, 57666-57670 (2015).
63. H. Y. Wang, B. Y. Wang, D. Wang, L. Lu, J. G. Wang, and Q. C. Jiang, Facile synthesis of hierarchical worm-like MoS_2 structures assembled with nanosheets as anode for lithium ion batteries, *RSC Adv.*, **5**, 58084-58090 (2015).
64. Y. Zhou, Y. Liu, W. Zhao, R. Xu, D. Wang, B. Li, X. Zhou, and H. Shen, Rational design and synthesis of 3D MoS_2 hierarchitecture with tunable nanosheets and 2H/1T phase within graphene for superior lithium storage, *Electrochim. Acta*, **211**, 1048-1055 (2016).
65. M. Wu, J. Zhan, K. Wu, Z. Li, L. Wang, B. Geng, L. Wang, and D. Pan, Metallic 1T MoS_2 nanosheet arrays vertically grown on activated carbon fiber cloth for enhanced Li-ion storage performance, *J. Mater. Chem. A*, **5**, 14061-14069 (2017).
66. T. Wang, C. Sun, M. Yang, G. Zhao, S. Wang, F. Ma, L. Zhang, Y. Shao, Y. Wu, B. Huang, and X. Hao, Phase-transformation engineering in MoS_2 on carbon cloth as flexible binder-free anode for enhancing lithium storage, *J. Alloys Compd.*, **716**, 112-118 (2017).
67. B. Chen, N. Zhao, L. Guo, F. He, C. Shi, C. He, J. Li, and E. Liu, Facile synthesis of 3D few-layered MoS_2 coated TiO_2 nanosheet core-shell nanostructures for stable and high-performance lithium-ion batteries, *Nanoscale*, **7**, 12895-12905 (2015).
68. M. Wang, L. Fan, D. Tian, X. Wu, Y. Qiu, C. Zhao, B. Guan, Y. Wang, N. Zhang, and K. Sun, Rational design of hierarchical SnO_2/1T-MoS_2 nanoarray electrode for ultralong-Life Li-S batteries, *ACS Energy Lett.*, **3**, 1627-1633 (2018).
69. Y. C. Jeong, J. H. Kim, S. H. Kwon, J. Y. Oh, J. Park, Y. Jung, S. G. Lee, S. J. Yang, and C. R. Park, Rational design of exfoliated 1T MoS_2@CNT-based bifunctional separators for lithium sulfur batteries, *J. Mater. Chem. A*, **5**, 23909-23918 (2017).

70. S. Dan, Y. Delai, L. Ping, T. Yougen, G. Jun, W. Lianzhou, and W. Haiyan, MoS_2/graphene nanosheets from commercial bulky MoS_2 and graphite as anode materials for high rate sodium ion batteries, *Adv. Energy Mater.*, **8**, 1702383-1702394 (2018).
71. Y. Li, Y. Liang, F. C. Robles Hernandez, H. D. Yoo, Q. An, and Y. Yao, Enhancing sodium-ion battery performance with interlayer-expanded Mo_3-PEO nanocomposites, *Nano Energy*, **15**, 453-461 (2015).
72. Y. L. Liang, H. D. Yoo, Y. F. Li, J. Shuai, H. A. Calderon, F. C. R. Hernandez, L. C. Grabow, and Y. Yao, Interlayer-expanded molybdenum disulfide nanocomposites for electrochemical magnesium storage, *Nano Lett.*, **15**, 2194-2202 (2015).
73. Y. Liu, L.-Z. Fan, and L. Jiao, Graphene intercalated in graphene-like MoS_2: A promising cathode for rechargeable Mg batteries, *J. Power Sources*, **340**, 104-110 (2017).